Ingenol mebutate signals via PKC/MEK/ERK in keratinocytes and induces interleukin decoy receptors IL1R2 and IL13RA2

Freiberger, Sandra N ; Cheng, Phil F ; Iotzova-Weiss, Guergana ; Neu, Johannes ; Liu, Qinxiu ; Dziunycz, Piotr ; Zibert, John R ; Dummer, Reinhard ; Skak, Kresten ; Levesque, Mitchell P ; Hofbauer, Günther F L

Abstract: Squamous cell carcinoma (SCC) is the second most common human skin cancer and the second leading cause of skin cancer-related death. Recently, a new compound, ingenol mebutate, was approved for treatment of actinic keratosis, a precursor of SCC. As the mechanism of action is poorly understood, we have further investigated the mechanism of ingenol mebutate-induced cell death. We elucidate direct effects of ingenol mebutate on primary keratinocytes, patient-derived SCC cells, and a SCC cell line. Transcriptional profiling followed by pathway analysis was performed on ingenol mebutate-treated primary keratinocytes and patient-derived SCC cells to find key mediators and identify the mechanism of action. Activation of the resulting pathways was confirmed in cells and human skin explants and supported by a phosphorylation screen of treated primary cells. The necessity of these pathways was demonstrated by inhibition of certain pathway components. Ingenol mebutate inhibited viability and proliferation of all keratinocyte-derived cells in a biphasic manner. Transcriptional profiling identified the involvement of PKC/MEK/ERK signaling in the mechanism of action and inhibition of this signaling pathway rescued ingenol mebutate-induced cell death after treatment with 100 nmol/L ingenol mebutate, the optimal concentration for the first peak of response. We found the interleukin decoy receptors IL1R2 and IL13RA2 induced by ingenol mebutate in a PKC/MEK/ERK-dependent manner. Furthermore, siRNA knockdown of IL1R2 and IL13RA2 partially rescued ingenol mebutate-treated cells. In conclusion, we have shown that ingenol mebutate-induced cell death is mediated through the PKC /MEK/ERK pathway, and we have functionally linked the downstream induction of IL1R2 and IL13RA2 expression to the reduced viability of ingenol mebutate-treated cells. Mol Cancer Ther; 14(9); 2132-42. ©2015 AACR.

DOI: https://doi.org/10.1158/1535-7163.MCT-15-0023-T

Ingenol mebutate signals via PKC/MEK/ERK in keratinocytes and induces interleukin decoy receptors IL1R2 and IL13RA2

Sandra N. Freiberger[1]; Phil F. Cheng[1]; Guergana Iotzova-Weiss [1]; Johannes Neu[1]; Qinxiu Liu[1]; Piotr Dziunycz[1]; John R. Zibert[2]; Reinhard Dummer[1]; Kresten Skak[2]; Mitchell P. Levesque[1]; Günther F.L. Hofbauer[1]*

[1] Department of Dermatology, University Hospital Zurich, Switzerland

[2] LEO Pharma A/S, Ballerup, Denmark

* Corresponding author: Günther F. L. Hofbauer, Department of Dermatology, University Hospital Zurich, Gloriastrasse 31, 8091 Zurich, Switzerland. Phone: +41 44 2551111; E-mail: Hofbauer@usz.ch

Running title: Ingenol mebutate's mechanism in keratinocytes

Keywords: cutaneous squamous cell carcinoma, ingenol mebutate, PKC, MAPK, interleukin decoy receptors

Financial support: LEO Pharma A/S supported this study with a research grant to G. F. L. Hofbauer.

Disclosure of potential conflict of interest: Kresten Skak and John Zibert are employees of LEO Pharma A/S.

Word count: 4631

Number of figures: 5 figures and 6 supplementary figures

Number of tables: 1 supplementary table

Abstract

Squamous cell carcinoma (SCC) is the second most common human skin cancer and the second leading cause of skin cancer-related death. Recently, a new compound, ingenol mebutate (IM), was approved for treatment of actinic keratosis (AK), a precursor of SCC. Since the mechanism of action is poorly understood, we have further investigated the mechanism of IM-induced cell death.

We elucidate direct effects of IM on primary keratinocytes, patient-derived SCC cells and a SCC cell line. Transcriptional profiling followed by pathway analysis was performed on IM-treated primary keratinocytes and patient-derived SCC cells to find key mediators and identify the mechanism of action. Activation of the resulting pathways was confirmed in cells and human skin explants and supported by a phosphorylation screen of treated primary cells. The necessity of these pathways was demonstrated by inhibition of certain pathway components.

IM inhibited viability and proliferation of all keratinocyte-derived cells in a biphasic manner. Transcriptional profiling identified the involvement of PKC/MEK/ERK signaling in the mechanism of action and inhibition of this signaling pathway rescued IM-induced cell death after treatment with 100 nM IM, the optimal concentration for the first peak of response. We found the interleukin decoy receptors IL1R2 and IL13RA2 induced by IM in a PKC/MEK/ERK-dependent manner. Furthermore, siRNA knock-down of *IL1R2* and *IL13RA2* partially rescued IM-treated cells.

In conclusion, we have shown that IM-induced cell death is mediated through the PKCδ/MEK/ERK pathway, and we have functionally linked the downstream induction of *IL1R2* and *IL13RA2* expression to the reduced viability of IM-treated cells.

Introduction

Actinic keratoses (AKs) are hyperkeratotic lesions on sun-exposed surfaces such as the face, scalp and lower arms. AKs are caused by accumulated UV exposure over lifetime and develop from atypically proliferating keratinocytes (1). In about 8% of cases, AKs can progress to invasive SCCs (2), the second most common form of skin cancer, and therefore need to be treated. About 50% of SCCs harbor p53 mutations, some of them with the typical UV signature of cyclobutane pyrimidine dimers (3). The risk for organ transplant recipients to develop SCC is highly increased due to their treatment with immunosuppressive drugs (4) such as azathioprine, a photosensitizer to UVA light (5) or cyclosporine A inducing the protumorigenic transcription factor ATF3 (6, 7). The incidence of SCC in the general population continues to increase with high morbidity and low mortality (8). In contrast to basal cell carcinoma (BCC), SCC carries a risk of metastasis. The current treatment options for actinic keratosis range from topical treatments with gels or creams for field cancerization to cryotherapy for single lesions (9), whereas SCC is normally treated by surgical excision. Self-directed treatments are preferred by patients, but are time consuming as they need to be applied for weeks or months to produce clinical results.

Recently a new compound, ingenol mebutate (IM), was registered in the USA and Europe for topical treatment of AK in two different concentrations depending on the treatment location. IM showed 42.2% complete clinical clearance compared to placebo (10) and has the great advantage of a short treatment duration (i.e. two to three consecutive days), a short period of local skin reaction and no systemic adverse events (11, 12). Although IM is registered and used in the clinic, its exact mechanism of action is not fully understood. Recent studies suggest a dual mechanism of action with rapid initial necrosis (13) followed by activation of the innate immune system (14). Although several reports investigated the mechanism of action of IM on different cancer cell lines like colon cancer (15), melanoma (16) and leukemia (17), there is only one report studying the effect on epithelial cells (18). In that paper, the authors demonstrate acute cytotoxicity of clinical drug concentrations on cancer cell lines and keratinocytes with disruption of the mitochondrial network and the involvement of intracellular calcium release.

To better characterize the mechanism of action of IM in epithelial cells, we analyzed the impact of IM on the proliferation and viability of primary keratinocytes, primary patient-derived SCC cells and a SCC cell line. Furthermore, we identified signaling pathways essential for IM action by gene expression analysis and confirmed their contribution in primary cell cultures and human skin explants. We functionally demonstrated the critical importance of several novel genes using functional *in vitro* assays.

Materials and Methods

Cell culture and skin explants

The human SCC12 cell line (19) was cultured in Keratinocyte-SFM supplemented with L-glutamine, EGF and BPE (Gibco, Basel, Switzerland). The human SCC13 cell line (19) was cultured in DMEM (Gibco) with 10% fetal calf serum (FCS). Both cell lines were obtained from Gian-Paolo Dotto (University of Lausanne) in 2011 and were not further tested. Human primary keratinocytes and fibroblasts were isolated from healthy human skin. Human fibroblasts and melanoma cells were cultured in RPMI 1640 (Sigma, Buchs, Switzerland) with 10% FCS. Melanoma cells were isolated from biopsies taken from consenting patients. Normal skin samples were obtained from abdominal and mammary surgery. Human primary SCC cells were isolated from punch biopsies taken from SCC surgical excisions. Both healthy skin and SCC biopsies were also used as whole explants for experiments. Primary cells were cultured in CnT-07 medium (CellNTec, Bern, Switzerland). All cells were cultured at 37°C and 5% CO_2.

Institutional board approval for the use of human tissue was granted; all donors signed written informed consent forms in accordance with the Code of Ethics of the World Medical Association (Declaration of Helsinki) for experiments involving humans (ethical approval number EK647). All samples were obtained from the University Hospital Zurich.

Viability and proliferation assay

Cells were seeded on 24- or 96-well plates at 50% confluence and treated for 24h with IM or DMSO, respectively. When indicated, IM and DMSO were combined with specific kinase inhibitors. Viability was analyzed by MTT assay (Sigma). Proliferation was assessed by BrdU incorporation using the BrdU assay kit (Merck Millipore, Darmstadt, Germany).

Gene expression array and analysis

Gene expression was analyzed in normal keratinocytes and patient-derived SCC cells 24h after IM or control treatment. RNA was isolated and cDNA was generated. The SurePrint G3 Human GE v2 8x60K Microarray (Agilent, Santa Clara, CA, United States) was used to analyze the samples.

Author Manuscript Published OnlineFirst on June 26, 2015; DOI: 10.1158/1535-7163.MCT-15-0023-T
Author manuscripts have been peer reviewed and accepted for publication but have not yet been edited.

Raw data was processed in the programming environment R using the limma package (20). The data were background corrected and quantile normalized. Pairwise comparison of treatment vs control samples was performed for each cell line. Differentially expressed genes were deemed to be significant if the absolute log-fold change was more than 2 and the FDR adjusted p-value was less than 0.05. Heat map was generated by hierarchical clustering and Euclidean distance was used for distance metric. Microarray data have been deposited in NCBI's Gene Expression Omnibus (21) in accordance with MIAME guidelines (GEO Series accession number GSE63308). Pathway analysis of deregulated genes was done using the software GeneGo (Thomson Reuters, Zug, Switzerland).

RNA isolation and qPCR

RNA from cells and tissue was isolated with TRIzol® (Invitrogen, Basel, Switzerland) as described in the protocol. Reverse transcription was achieved using the Reverse Transcription Kit from Promega (Madison, WI, United States). qPCR was performed on the ViiA7 real time PCR machine (life technologies, Zug, Switzerland) using SYBR green mix (Roche, Basel, Switzerland). The following primers from Microsynth (Balgach, Switzerland) were used.

36B4 fwd: 5'-GCAATGTTGCCAGTGTCTGT-3', *36B4* rev: 5'-GCCTTGACCTTTTCAGCAAG-3'

IL1R2 fwd: 5'-CAGCTTCTCTGGGGTCAAGA-3', *IL1R2* rev: 5'-CGTGGCCCCTCGGTCA-3'

IL13RA2 fwd: 5'-GCGGGGAGAGAGGCAATATC-3', *IL13RA2* rev: 5'-AGCATCCGATAGCCAAGCAA-3'

PKCδ fwd: 5'-CTGCAAGAAGAACAATGGCAAG-3', *PKCδ* rev: 5'-ATCCACGTCCTCCAGGAAATACT-3'

DEFB4A fwd: 5'-TGGTGAAGCTCCCAGCCATC-3', *DEFB4A* rev: 5'-ATACCACCAAAAACACCTGGAAGA-3'

C15orf48: 5'-CCCACCAGGCGATCAATACT-3', *C15orf48* rev: 3'-AGGGAATGAGTTCCTTCCTTTTCA-3'

EGR1 fwd: 5'-ACCTGACCGCAGAGTCTTTT-3', *EGR1* rev: 5'-GAGTGGTTTGGCTGGGGTAA-3'

SPRY2 fwd: 5'-TGCACATCGCAGAAAGAAGAG-3', *SPRY2* rev: 5'-AGAACACATCTGAACTCCGTGA-3'

CFOS fwd: 5'-GGGGCAAGGTGGAACAGTTA-3', *CFOS* rev: 5'-AGTTGGTCTGTCTCCGCTTG-3'

Protein detection

Cells were lysed in RIPA buffer (Cell Signaling, Danvers, MA, United States, #9806) and protein extracts were analyzed by western blotting using the following antibodies: anti-pPKCδ T505 (#9374), anti-pPKCδ

Y311 (#2055), anti-PKCδ (#9616), anti-pPKCα/βII T638/641 (#9375), anti-PKCα (#2056) anti-pp42/44 (#9101), anti-p42/44 (#9102), anti-pJNK (#9251), anti-JNK (#9252), anti-pp38 (#9211), anti-p38 (#9212), anti-rabbitHRP (#7074) all from Cell Signaling, anti-β-Actin (sc-47778, Santa Cruz Biotechnologies, Heidelberg, Germany), Rabbit anti-mouse IgG H&L HRP (ab6728). Proteins were detected by ECL on Hyperfilm (Amersham, GE Healthcare, Glattbrugg, Switzerland).

Phosphoprotein array

PathScan® Intracellular Signaling Array Kit from Cell Signaling (#7323) was used according to the manufacturer's instructions.

Drugs and inhibitors

Ingenol mebutate (Suppl. Fig. 1A) was kindly provided by LEO Pharma A/S (Ballerup, Denmark). Ingenol mebutate was either dissolved in DMSO for cell culture treatment or suspended in commercial vehicle for treatment of organ cultures. Cells and organ cultures were treated with different drug concentrations for varying durations as indicated. For PKC inhibition, AEB071 (Selleckchem, Houston, TX, United States, S2791) was used at concentrations between 500 nM and 10 μM. The ERK inhibitor SCH772984 (ChemScene, Monmouth Junction, NJ, United States, CS-1421) and the MEK inhibitor GSK1120212 (Cellagen Technology, San Diego, United States, #C4112-5) (Suppl. Fig. 1B) were used at concentrations of 500 nM. The JNK inhibitor SP600125 (Santa Cruz, sc-200635) was used at 100-500 nM. The p38 inhibitor SB203580 (Cell Signaling, #5633) was used at 250-500 nM. 12-O-Tetradecanoylphorbol-13-acetate (TPA) (Sigma, #P1585) and used at various concentrations as indicated in the results section.

Knock-down

For knock down of *PKCδ*, *IL1R2*, and *IL13RA2*, cells were transfected with INTERFERin® (Polyplus transfections) and specific siRNAs (QIAgen, Hombrechtikon, Switzerland).

siCtrl: target sequence 5'-AATTCTCCGAACGTGTCACGT-3'

siPKCα #3: target sequence 5'-CAAGACGTCTTTGGAATCCAA-3'

siPKCα #5: target sequence 5'-AACCATCCGCTCCACACTAAA -3'

si*PKCδ* #1: target sequence 5'-CCGGGACACTATATTCCAGAA-3'

si*PKCδ* #7: target sequence 5'-AACTCTACCGTGCCACGTTTT-3'

si*PKCδ* #11: target sequence 5'-CAGCAGCAAGTGCAACATCAA-3'

si*IL1R2* #2: target sequence 5'-CACGCCAGGAATATTCAGAAA-3'

si*IL1R2* #4: target sequence 5'-AAGACTGACAATCCCGTGTAA -3'

si*IL13RA2* #1: target sequence 5'-CAGGATATGGATTGCGTATAT-3';

si*IL13RA2* #5: target sequence 5'-AAGGTGAAGACCTATCGAAGA-3'

Cells were incubated for 30h with the transfection mix before they were treated with the drug for 24h. Knock-down of each gene was confirmed (Suppl. Fig. 2).

Immunohistochemistry

After treatment samples were fixed in 4% formalin for 2 days, followed by dehydration and embedding in paraffin. Seven µm sections were made and stained with H&E or for pERK with the antibody pp42/44 (Cell Signaling, #9101).

Results

Ingenol mebutate inhibits viability and proliferation of keratinocytes and SCC cells

To investigate the impact of IM on epithelial cell viability and proliferation and to determine a working concentration for further experiments, we treated primary keratinocytes, patient-derived SCC cells, and SCC cell lines for 24h, 48h and 72h with IM in a range from 1 nM to 10^5 nM. All cell types showed a biphasic decrease in viability (Fig. 1A) and proliferation (Fig. 1B) upon drug treatment. Interestingly, all cells exhibited a drop in viability and proliferation around a concentration of 100 nM, while cells appeared healthier at lower (1-10 nM) and higher (10^3-10^4 nM) concentrations (Fig. 1A and 1B). At a concentration of 10^5 nM, cells died to a great extent due to cytotoxicity. For further experiments we used a concentration of 100 nM, since this concentration had the largest effect at the first peak of the biphasic response.

To find out whether the biphasic effect was cell-type specific, we additionally treated fibroblasts and melanoma cells with similar concentrations of IM for 24h. We found no biphasic effect in fibroblasts, since they were resistant to the highest concentration used (10^5 nM). Melanoma cells did not show a biphasic effect either, since they were almost unaffected at low concentrations, whereas viability was 50% decreased at the highest concentration used in the experiment (10^5 nM) (Suppl. Fig. 3A). Furthermore, we analyzed the viability of the SCC13 cell line after 24h treatment with several concentrations of the tumor promoting tetradecanoyl phorbol acetate (TPA), a drug structurally related to the anti-cancer drug IM, both being phorbol esters and known potent PKC activators (22). This was done to investigate if the effect observed with IM was drug- specific. Unlike IM we did not detect any biphasic effect upon TPA treatment (Suppl. Fig. 3B).

Gene expression analysis reveals involvement of PKC and MAPK signaling

To identify genes and signaling pathways mediating IM activity, we performed gene expression analysis on primary keratinocytes and patient-derived SCC cells treated for 24h with either DMSO or different concentrations of IM (1 nM, 100 nM, 10^4 nM). In concordance with the results from the viability and proliferation assays, most genes were differentially expressed in the presence of 100 nM IM (Fig. 2A). Fewer changes were detected at a concentration of 10^4 nM while 1 nM of IM had almost no effect (Suppl.

Fig. 4A). At a concentration of 100 nM, we found 1227 genes upregulated in keratinocytes and 795 in SCC cells. 390 of these genes overlap between the two cell types. Furthermore, we found 1887 downregulated genes in keratinocytes and 996 in SCC cells with 713 genes overlapping (Fig. 2B). Hierarchical clustering of the microarray data showed common clusters of gene expression patterns in the keratinocytes and SCC cells upon drug treatment, as compared to vehicle-treated cells. Pathway analysis of down-regulated genes using the software GeneGo identified mostly cell cycle-associated pathways and DNA damage repair pathways (Suppl. Fig. 4B). Upregulated genes following 100 nM IM treatment mostly affected pathways such as ERK1/2- and Protein Kinase C (PKC)-signaling in keratinocytes and ERK1/2 signaling in SCC cells (Suppl. Fig. 4C).

To identify key mediators of the IM effect, we took the top 5 upregulated genes in SCC cells that were also upregulated in keratinocytes. *DEFB4A*, *ZP4*, *IL13RA2*, *CCL5*, and *IL1R2* were thus selected. We did not focus on C15orf48, which was also was among the top 5 upregulated genes, since we were interested in genes that are upregulated in both healthy and cancerous keratinocytes and C15orf48 was only found to be upregulated in SCC cells. Furthermore, we could not confirm the upregulation of C15orf48 in SCC tissue (data not shown). From literature research, we found DEFB4A, IL1R2 and IL13RA2 to be the most interesting ones. IL1R2 and IL13RA2 are decoy receptors that were thought to have no signaling function. However, a recent paper demonstrated a signaling ability of IL13RA2 (23). Additionally, IL13AR2 was reported to slow down or even prevent tumor growth in mice when overexpressed in pancreatic or breast cancer cells (24). Furthermore, IL1β was shown to enhance proliferation of oral keratinocytes (25) and therefore the upregulation of its decoy receptor by IM may play a crucial role in the mechanism of action of IM. DEFB4A was shown to be differentially expressed in SCC (26). We then confirmed the upregulation of these genes by qPCR in keratinocytes, patient-derived SCC cells, two SCC cell lines, human epidermis and human SCC explants after 24h of IM treatment. We found *IL1R2* and *IL13RA2* consistently and significantly upregulated in all tested cell types and explant tissues after treatment with IM, while *DEFB4A* upregulation could not be confirmed in SCC cell lines and SCC explants (Suppl. Fig. 4D, Suppl. Tab. 1).

PKCδ plays a fundamental role in the mechanism of action of ingenol mebutate

As our pathway analysis agreed with earlier studies (16, 22) that indicated a role for PKC signaling following IM exposure, we further investigated this pathway as a possible mechanism of action in the loss

of epithelial cell viability and proliferation. We incubated primary keratinocytes, patient-derived SCC cells and the SCC13 cell line with 100 nM IM for up to 45 minutes and found PKCδ to be highly phosphorylated in the hinge region (Y311) in all cell types while PKCα is not phosphorylated (Fig. 3A). Y311 was previously reported to be required for PKCδ activation and furthermore enhances autophosphorylation of PKCδ on T505 (27). Accordingly, we found the activation loop (T505) of PKCδ to be more phosphorylated in all three cell types after 24h drug treatment, whereas this phosphorylation could be blocked by the PKC inhibitor AEB071 (Fig. 3B). Although PKCδ can function without being phosphorylated at T505, this phosphorylation increases the catalytic activity of PKCδ (27). Furthermore, T505 phosphorylation influences the substrate specifity of PCKδ and is essential for the activation of the AP1 family of transcription factors (28).

To further investigate the role of PKCδ, we used IM alone or in combination with the PKC inhibitor AEB071 and measured cell viability of primary keratinocytes, SCC patient cells and the SCC13 cell line after 24h of treatment. We found cell viability to be partially rescued by PKC inhibition when treated with IM (Fig. 3C). Since the PKC inhibitor is not entirely specific for single isoforms, we further validated the role of PKCδ using siRNA to knock-down PKCδ in SCC13 cells followed by analysis of cell viability after 24h IM treatment. Similar to our findings with the PKC inhibitor, we detected a rescue of cell viability upon IM treatment when PKCδ was knocked down. A knock-down PKCα followed by IM treatment led only to a partial rescue, while PKCδ knock-down could rescue the IM-treated cells completely (Fig. 3D).

ERK is activated by ingenol mebutate treatment in a PKC-dependent manner and mediates IM-dependent effects on cell viability

Besides PKC signaling, our pathway analysis suggested ERK1/2 to be involved in mediating the effect of IM. To confirm this and to exclude other pathways involved in MAPK signaling (e.g. p38, JNK) we performed a phosphorylation array experiment with primary keratinocytes and SCC cells from three different donors and found ERK to be phosphorylated upon IM treatment, while other pathways of MAPK signaling (p38 and JNK) showed no or only weak phosphorylation (Suppl. Fig. 5A). Weak or nonexistent phosphorylation of JNK and p38 was further validated on cells from more donors by conventional western blotting (Fig. 4A). In order to test the effect of IM in a more natural model of skin, we treated human skin

explants in three independent experiments with either vehicle or IM gel 0.05%. Assessment of ERK phosphorylation after 24h of treatment revealed a sustained activation of ERK compared to vehicle-treated samples (Fig. 4B). To further demonstrate activation of ERK, we analyzed the expression of known ERK target genes (*EGR1*, *SPRY2*, *CFOS*) (29) in SCC13 cells, primary keratinocytes and patient-derived SCC cells after 24h of treatment by qPCR and found them to be upregulated upon IM treatment, while the upregulation of the ERK target genes was abolished by an ERK inhibitor (SCH772984) and a MEK inhibitor (GSK1120212B) (Suppl. Fig. 5B). Additionally, we used either the PKC inhibitor AEB071 or a knock-down of PKCδ, either alone or in combination with IM and analyzed the expression of ERK target genes. Either inhibition of PKC or knock-down of PKCδ could prevent the upregulation of ERK target gene expression after IM treatment (Fig. 4C). Furthermore, we analyzed the phosphorylation of ERK by western blotting after short-term IM treatment in cells treated with the PKC inhibitor and in cells with PKCδ knock-down. The drug alone induced phosphorylation of ERK, which was blocked by addition of the PKC inhibitor (Fig. 4D, left panel) or by knock-down of PKCδ (Fig. 4D, right panel). This was confirmed in human skin explants pre-incubated in either DMSO or PKC inhibitor for 2h and treated with either vehicle or IM gel 0.015%. After 18h of incubation we analyzed pERK status by immunohistochemistry and found sustained ERK phosphorylation after drug treatment, while this phosphorylation was abolished by the PKC inhibitor (Fig. 4E). Taken together these results indicate that ERK is rapidly phosphorylated by IM in a PKC-dependent manner upon drug treatment. To further investigate these pathways in the mechanism of action of IM we analyzed the viability of primary keratinocytes, patient-derived SCC cells and the SCC13 cell line after 24h treatment with either the drug alone or in combination with the ERK inhibitor (SCH772984) or the MEK inhibitor (GSK1120212B). As seen in previous experiments, cell viability dropped below 50% upon IM treatment. However, viability was partially rescued when cells were treated in combination with the MEK or ERK inhibitor but not in combination with the JNK inhibitor SP600125 or the p38 inhibitor SB203580 (Fig. 4F).

IL1R2 and IL13RA2 partially mediate the mechanism of action of ingenol mebutate in SCC

To further investigate the role of *IL1R2* and *IL13RA2*, we first confirmed their upregulation upon 24h IM treatment in keratinocytes, patient-derived SCC cells, the SCC12 and SCC13 cell lines and epidermis from human explants by qPCR (Suppl. Fig. 4D). *C15orf48* was not further investigated due to the lack of a

commercially available antibody and the fact that we could not confirm its upregulation in SCC tissue. Since we saw an upregulation of *IL1R2* and *IL13RA2* after 24h of treatment, we performed time course experiments in primary keratinocytes and epidermis from human skin explants to better define the timescale of gene regulation. We found both genes to be upregulated after 2-6h of treatment (Suppl. Fig. 6).

Furthermore we treated cells with IM alone or in combination with the PKC-, the MEK- or the ERK inhibitor respectively and found that the drug-dependent upregulation of both genes was partially abolished. IM in combination with JNK inhibition or p38 inhibition had almost no repressive effect on the expression of the two genes (Fig. 5A). Additionally we knocked down PKCδ by siRNA, which also prevented the drug-dependent upregulation of *IL1R2* and *IL13RA2* mRNA (Fig. 5B). To find out whether *IL1R2* or *IL13RA2* play an essential role in the mechanism of action IM, we knocked down these two genes with siRNA and analyzed cell viability upon drug treatment. Interestingly, both *IL1R2* and *IL13RA2* knock down partially rescued the viability of drug-treated SCC13 cells (Fig. 5C).

Discussion

Ingenol mebutate (IM) is approved for the topical treatment of actinic keratosis (AK), the precursor of squamous cell carcinoma (SCC). However, its mechanism of action is not completely understood. Several studies investigated IM in the context of different cancers (15-17) and suggest a role of the innate immune system (14) but there is only one study that focuses on the effect on the actual target, the malignant keratinocytes (18). While that study used high IM concentrations (100-400 µM) and short incubation times, leading to cytotoxicity involving mitochondrial network disruption, we investigated the mechanism of action of IM in healthy keratinocytes, SCC cells and skin explants at lower concentrations (100 nM) and up to 72h. We showed that IM induced a direct effect on viability and proliferation on cells of different origin. Previous studies on different mouse and human cancer cell lines, like melanoma or breast carcinoma, determined the lethal dose (LD90) of IM for these cells to be between 180 and 220 µM after 24h (13). Benhadji *et al*. assessed growth inhibition by MTT assay and calculated the IC50 of colon cancer cell lines, finding great variations from 3 µM in Colo-205 cells to more than 300 µM in HCT116 and HCC2998 cells (30). Overall the concentrations leading to cell death strongly vary depending on the cell line tested and our results fit within this range showing most cells reaching a lethal affect at 100 µM IM. In line with other reports (16), we found fibroblasts to be relatively resistant to IM while melanoma cells were affected, but at higher concentrations than the keratinocytes. In contrast to melanoma cells and fibroblasts, we found a biphasic effect on viability and proliferation on keratinocytes and SCC cells. This determines that IM induces cell death in two ways, depending on concentration and cell type. Furthermore, our results on SCC13 cells indicated that the biphasic effect was IM-specific as compared to another PKC activator, TPA. Our microarray performed with various IM concentrations showed the highest number of genes differentially expressed at 100 nM, whereas effects were less pronounced at lower and higher concentrations, consistent with the impact of 100 nM IM on cell viability and proliferation. This pronounced effect at 100 nM again points to the existence of two different concentration-dependent mechanisms of action for IM, whereas the highest concentration used leads to cell death due to direct cytotoxicity. The lower concentration of 100 nM however, may trigger intracellular pathways that lead to the reduction of cell viability. These potential signaling pathways were subject to our further investigations.

PKCδ is a key mediator in cell differentiation and inhibition of proliferation in various tissues (31-34). A direct binding of IM to PKC isoforms has been observed (22). IM treatment leads to phosphorylation of PKCδ in the Colo-205 cancer cell line (30). In other studies, PKCδ was reported to drive keratinocyte differentiation and inhibit proliferation of the immortalized keratinocyte line HaCaT, which could be reversed by PKCδ inhibition (32). Our data from gene expression to functional experiments in primary cell cultures underline a critical role for PKCδ in mediating the effect of IM in keratinocytes and verify such previous observations correspondingly for IM while PKCα played only a minor role in our setting.

Downstream of PKC signaling, our pathway analysis revealed an involvement of ERK1/2 in the mechanism of action of IM. Previous work on colon cancer cells suggests involvement of MAPK pathways including JNK and p38 (30, 35) by showing phosphorylation of these proteins after IM treatment. We confirmed activation of ERK1/2 while we were able to exclude a major role of other MAPK pathway components like JNK and p38 in keratinocytes and SCC cells. Similar to previous studies on melanoma cells (16), our data on keratinocytes clearly link PKCδ to the activation of MAPK signaling. Both MEK and ERK are essential for the effect of IM in our assays. Although the activation of the MEK/ERK pathway is generally considered to promote tumor cell growth (36), ERK activation seems to contribute favorably to the mechanism of action of IM, leading to reduced cell viability and proliferation. In line with this assumption, ERK activation was found to suppress tumors by promotion of selective protein degradation (37). Moreover, high ERK activation can serve as a marker of improved outcome in breast cancer patients (38).

We identified and validated a role for several novel genes as critical players in the mechanism of action of IM. Our analysis focused on *IL13RA2* and *IL1R2*, which were both induced by IM in a PKCδ/MEK/ERK-dependent manner. Both genes encode for interleukin receptors that are commonly known to function as decoy receptors without signaling ability (39, 40). Nevertheless, a recent publication attributed an active role to *IL13RA2* in signaling, thus inducing TGFβ-mediated fibrosis (23). However, to the case for IM induced effects, induction of fibrosis is unlikely as patients treated with IM do not show (fibrosis-related) scarring and have a good cosmetic outcome post-treatment with IM gel (11). Moreover, a recent study

revealed a role of IL13RA2 in tumor suppression, as IL13RA2-overexpressing breast and pancreatic cancer cells showed reduced or no tumor growth when injected into mice (24).

Similarly, *IL1R2* recently showed activity against ectopic tissue growth and endometriosis progression and could down-regulate the anti-apoptotic protein Bcl2 (41), which could explain that the cell death mechanism by IM could be attributed by IL1R2 signaling. As IL1β was shown to promote proliferation of oral keratinocytes (25), one could speculate whether IL1R2 is upregulated by IM to capture IL1β and prevent this effect. Further studies are needed to clarify the role of *IL13RA2* and *IL1R2* in the mechanism of action of IM.

In summary, we report a mechanism of action for IM in proliferating normal and malignant keratinocytes through specific activation of PKCδ leading to activation of MEK/ERK signaling, resulting in decreased viability. This was dependent on concentration and cell type, resulting in a unique biphasic induced loss of viability through IM. A set of genes responsive to IM treatment, mainly *IL13RA2* and *IL1R2*, showed that they partially mediate the function of IM on SCC, suggesting a function for them apart from their role in the immune system. However, our data do not allow us to conclude whether *IL13RA2* and *IL1R2* exert their effect primarily in keratinocytes treated by IM or whether they are instrumental in orchestrating the accompanying immune response. Further projects are needed to shed more light on this matter.

Acknowledgements

The gene expression array was done by the Functional Genomic Center Zurich (FGCZ). The authors thank Ines Kleiber-Schaaf (Dept. of Dermatology, University Hospital Zurich) for immunohistochemical staining. The University Research Priority Program in translational cancer research at the University of Zurich provided melanoma and fibroblast cultures used here.

References

1. Ackerman AB, Mones JM. Solar (actinic) keratosis is squamous cell carcinoma. Br J Dermatol. 2006;155:9-22.

2. Glogau RG. The risk of progression to invasive disease. J Am Acad Dermatol. 2000;42:23-4.

3. Brash DE, Rudolph JA, Simon JA, Lin A, McKenna GJ, Baden HP, et al. A role for sunlight in skin cancer: UV-induced p53 mutations in squamous cell carcinoma. Proc Natl Acad Sci U S A. 1991;88:10124-8.

4. Euvrard S, Kanitakis J, Claudy A. Skin cancers after organ transplantation. N Engl J Med. 2003;348:1681-91.

5. Hofbauer GF, Attard NR, Harwood CA, McGregor JM, Dziunycz P, Iotzova-Weiss G, et al. Reversal of UVA skin photosensitivity and DNA damage in kidney transplant recipients by replacing azathioprine. Am J Transplant. 2012;12:218-25.

6. Wu X, Nguyen BC, Dziunycz P, Chang S, Brooks Y, Lefort K, et al. Opposing roles for calcineurin and ATF3 in squamous skin cancer. Nature. 2010;465:368-72.

7. Dziunycz PJ, Lefort K, Wu X, Freiberger SN, Neu J, Djerbi N, et al. The oncogene ATF3 is potentiated by cyclosporine A and ultraviolet light A. J Invest Dermatol. 2014;134:1998-2004.

8. Hollestein LM, de Vries E, Nijsten T. Trends of cutaneous squamous cell carcinoma in the Netherlands: increased incidence rates, but stable relative survival and mortality 1989-2008. Eur J Cancer. 2012;48:2046-53.

9. Lazareth V. Management of non-melanoma skin cancer. Semin Oncol Nurs. 2013;29:182-94.

10. Lebwohl M, Swanson N, Anderson LL, Melgaard A, Xu Z, Berman B. Ingenol mebutate gel for actinic keratosis. N Engl J Med. 2012;366:1010-9.

11. Siller G, Gebauer K, Welburn P, Katsamas J, Ogbourne SM. PEP005 (ingenol mebutate) gel, a novel agent for the treatment of actinic keratosis: results of a randomized, double-blind, vehicle-controlled, multicentre, phase IIa study. Australas J Dermatol. 2009;50:16-22.

12. Siller G, Rosen R, Freeman M, Welburn P, Katsamas J, Ogbourne SM. PEP005 (ingenol mebutate) gel for the topical treatment of superficial basal cell carcinoma: results of a randomized phase IIa trial. Australas J Dermatol. 2010;51:99-105.

13. Ogbourne SM, Suhrbier A, Jones B, Cozzi SJ, Boyle GM, Morris M, et al. Antitumor activity of 3-ingenyl angelate: plasma membrane and mitochondrial disruption and necrotic cell death. Cancer Res. 2004;64:2833-9.

14. Challacombe JM, Suhrbier A, Parsons PG, Jones B, Hampson P, Kavanagh D, et al. Neutrophils are a key component of the antitumor efficacy of topical chemotherapy with ingenol-3-angelate. J Immunol. 2006;177:8123-32.

15. Ghoul A, Serova M, Astorgues-Xerri L, Bieche I, Bousquet G, Varna M, et al. Epithelial-to-mesenchymal transition and resistance to ingenol 3-angelate, a novel protein kinase C modulator, in colon cancer cells. Cancer Res. 2009;69:4260-9.

16. Cozzi SJ, Parsons PG, Ogbourne SM, Pedley J, Boyle GM. Induction of senescence in diterpene ester-treated melanoma cells via protein kinase C-dependent hyperactivation of the mitogen-activated protein kinase pathway. Cancer Res. 2006;66:10083-91.

17. Olsnes AM, Ersvaer E, Ryningen A, Paulsen K, Hampson P, Lord JM, et al. The protein kinase C agonist PEP005 increases NF-kappaB expression, induces differentiation and increases constitutive chemokine release by primary acute myeloid leukaemia cells. Br J Haematol. 2009;145:761-74.

18. Stahlhut M, Bertelsen M, Hoyer-Hansen M, Svendsen N, Eriksson AH, Lord JM, et al. Ingenol mebutate: induced cell death patterns in normal and cancer epithelial cells. J Drugs Dermatol. 2012;11:1181-92.

19. Rheinwald JG, Beckett MA. Tumorigenic keratinocyte lines requiring anchorage and fibroblast support cultured from human squamous cell carcinomas. Cancer Res. 1981;41:1657-63.

20. Smyth GK. Linear models and empirical bayes methods for assessing differential expression in microarray experiments. Stat Appl Genet Mol Biol. 2004;3:Article3.

21. Long X, Tharp DL, Georger MA, Slivano OJ, Lee MY, Wamhoff BR, et al. The smooth muscle cell-restricted KCNMB1 ion channel subunit is a direct transcriptional target of serum response factor and myocardin. J Biol Chem. 2009;284:33671-82.

22. Kedei N, Lundberg DJ, Toth A, Welburn P, Garfield SH, Blumberg PM. Characterization of the interaction of ingenol 3-angelate with protein kinase C. Cancer Res. 2004;64:3243-55.

23. Fichtner-Feigl S, Strober W, Kawakami K, Puri RK, Kitani A. IL-13 signaling through the IL-13alpha2 receptor is involved in induction of TGF-beta1 production and fibrosis. Nat Med. 2006;12:99-106.

24. Kawakami K, Kawakami M, Snoy PJ, Husain SR, Puri RK. In vivo overexpression of IL-13 receptor alpha2 chain inhibits tumorigenicity of human breast and pancreatic tumors in immunodeficient mice. J Exp Med. 2001;194:1743-54.

25. Lee CH, Chang JS, Syu SH, Wong TS, Chan JY, Tang YC, et al. IL-1beta promotes malignant transformation and tumor aggressiveness in oral cancer. J Cell Physiol. 2015;230:875-84.

26. Yoshimoto T, Yamaai T, Mizukawa N, Sawaki K, Nakano M, Yamachika E, et al. Different expression patterns of beta-defensins in human squamous cell carcinomas. Anticancer Res. 2003;23:4629-33.

27. Steinberg SF. Distinctive activation mechanisms and functions for protein kinase Cdelta. Biochem J. 2004;384:449-59.

28. Liu Y, Belkina NV, Graham C, Shaw S. Independence of protein kinase C-delta activity from activation loop phosphorylation: structural basis and altered functions in cells. J Biol Chem. 2006;281:12102-11.

29. Dieckgraefe BK, Weems DM. Epithelial injury induces egr-1 and fos expression by a pathway involving protein kinase C and ERK. Am J Physiol. 1999;276:G322-30.

30. Benhadji KA, Serova M, Ghoul A, Cvitkovic E, Le Tourneau C, Ogbourne SM, et al. Antiproliferative activity of PEP005, a novel ingenol angelate that modulates PKC functions, alone and in combination with cytotoxic agents in human colon cancer cells. Br J Cancer. 2008;99:1808-15.

31. Zhang H, Okamoto M, Panzhinskiy E, Zawada WM, Das M. PKCdelta/midkine pathway drives hypoxia-induced proliferation and differentiation of human lung epithelial cells. Am J Physiol Cell Physiol. 2014;306:C648-58.

32. Papp H, Czifra G, Bodo E, Lazar J, Kovacs I, Aleksza M, et al. Opposite roles of protein kinase C isoforms in proliferation, differentiation, apoptosis, and tumorigenicity of human HaCaT keratinocytes. Cell Mol Life Sci. 2004;61:1095-105.

33. Hernandez-Maqueda JG, Luna-Ulloa LB, Santoyo-Ramos P, Castaneda-Patlan MC, Robles-Flores M. Protein kinase C delta negatively modulates canonical Wnt pathway and cell proliferation in colon tumor cell lines. PLoS One. 2013;8:e58540.

34. Bowles DK, Maddali KK, Dhulipala VC, Korzick DH. PKCdelta mediates anti-proliferative, pro-apoptic effects of testosterone on coronary smooth muscle. Am J Physiol Cell Physiol. 2007;293:C805-13.

35. Serova M, Ghoul A, Benhadji KA, Faivre S, Le Tourneau C, Cvitkovic E, et al. Effects of protein kinase C modulation by PEP005, a novel ingenol angelate, on mitogen-activated protein kinase and phosphatidylinositol 3-kinase signaling in cancer cells. Mol Cancer Ther. 2008;7:915-22.

36. Pritchard AL, Hayward NK. Molecular pathways: mitogen-activated protein kinase pathway mutations and drug resistance. Clin Cancer Res. 2013;19:2301-9.

37. Deschenes-Simard X, Gaumont-Leclerc MF, Bourdeau V, Lessard F, Moiseeva O, Forest V, et al. Tumor suppressor activity of the ERK/MAPK pathway by promoting selective protein degradation. Genes Dev. 2013;27:900-15.

38. Svensson S, Jirstrom K, Ryden L, Roos G, Emdin S, Ostrowski MC, et al. ERK phosphorylation is linked to VEGFR2 expression and Ets-2 phosphorylation in breast cancer and is associated with tamoxifen treatment resistance and small tumours with good prognosis. Oncogene. 2005;24:4370-9.

39. Bernard J, Treton D, Vermot-Desroches C, Boden C, Horellou P, Angevin E, et al. Expression of interleukin 13 receptor in glioma and renal cell carcinoma: IL13Ralpha2 as a decoy receptor for IL13. Lab Invest. 2001;81:1223-31.

40. Colotta F, Re F, Muzio M, Bertini R, Polentarutti N, Sironi M, et al. Interleukin-1 type II receptor: a decoy target for IL-1 that is regulated by IL-4. Science. 1993;261:472-5.

41. Khoufache K, Bondza PK, Harir N, Daris M, Leboeuf M, Mailloux J, et al. Soluble human IL-1 receptor type 2 inhibits ectopic endometrial tissue implantation and growth: identification of a novel potential target for endometriosis treatment. Am J Pathol. 2012;181:1197-205.

Figure legend

Figure 1. Ingenol mebutate affects viability and proliferation of keratinocytes and SCC cells. Primary keratinocytes and patient-derived SCC cells of three different donors and the human squamous cell carcinoma cell lines SCC12 and SCC13 were treated with the indicated concentrations of ingenol mebutate for 24h, 48h or 72h. A, cell viability measured by MTT assay B, cell proliferation measured by BrdU incorporation. All values were normalized to DMSO-treated cells. Graphs represent mean and standard deviation of three independent experiments.

Figure 2. Gene expression analysis of IM-treated primary keratinocytes and patient-derived SCC cells. A, Heatmap showing triplicates of differentially expressed genes between DMSO-treated and IM-treated primary keratinocytes and patient-derived SCC cells. Cells were treated with either DMSO or 100 nM IM for 24h followed by RNA extraction and performance of the microarray. B, Number of differentially expressed genes in primary keratinocytes and patient-derived SCC cells after treatment with 100 nM IM. Upregulated genes are displayed in red, downregulated genes are displayed in blue.

Figure 3. PKCδ is phosphorylated after IM treatment and is essential for the performance of IM. A, Primary keratinocytes and SCC13 cells were treated with 100 nM IM for 10 min, 30 min or 45 min followed by protein extraction. Phosphorylation of PKCδ Y311 and PKCα/βII T638/641 was detected by western blotting. Total PKCδ or PKCα was used as loading control. B, Primary keratinocytes, patient-derived SCC cells and SCC13 cells were treated for 24h with 100 nM IM alone or in combination with the PKC inhibitor AEB071 followed by protein extraction. Phosphorylation of PKCδ T505 was detected by western blotting. Total PKCδ was used as loading control. C, Primary keratinocytes, patient-derived SCC cells and SCC13 cells were treated for 24h with 100 nM IM alone or in combination with the PKC inhibitor AEB071 followed by assessing cell viability by MTT assay. Graphs represent mean and sd of three independent experiments. Data were analyzed by one-way ANOVA followed by Dunnet's multiple-comparison test. * = $p<0.05$, ** = $p<0.01$, *** = $p<0.001$, **** = $p<0.0001$. D, SCC13 cells were transfected with two different siRNA against PKCδ (left panel) or PKCα (right panel) followed by 24h treatment with 100 nM IM and followed by assessing cell viability by MTT assay. Graphs represent mean and SD of three independent

experiments. Data were analyzed by Student's t-test. * = p<0.05, ** = p<0.01, *** = p<0.001, **** = p<0.0001.

Figure 4. ERK is activated by IM treatment in a PKC-dependent manner. A, Phosphorylation of JNK and p38 was analyzed in total protein extracts of primary keratinocytes and patient-derived SCC cells after 10 min and 30 min of IM treatment. B, Immunohistochemical staining for ERK phosphorylation after 24h treatment with either vehicle or IM 0.05% in healthy skin organ cultures from three different donors. Scale bar = 100 µm. C, ERK target genes are upregulated after 24h of IM treatment and can be blocked by PKC inhibition or by knockdown of PKCδ. Gene expression was assessed by qPCR. Graphs represent mean and SD of three independent experiments. Data were analyzed by one-way ANOVA followed by Dunnet's multiple-comparison test. * = p<0.05, ** = p<0.01, *** = p<0.001, **** = p<0.0001. D, Phosphorylation of ERK after IM treatment can be blocked by the PKC inhibitor or by knockdown of PKCδ. Primary keratinocytes, patient-derived SCC cells and SCC13 cells were treated for 10 min with IM alone or in combination with the PKC inhibitor followed by protein extraction. Moreover, SCC13 cells were transfected with two different siRNAs against PKCδ followed by 10 min IM treatment. Extracts were analyzed by western blotting and stained for ERK phosphorylation. Total ERK protein was used as loading control. E, Immunohistochemical staining of healthy skin for ERK phosphorylation after 18h treatment with either vehicle or IM 0.015% alone or in combination with the PKC inhibitor. Pictures show representative staining. Left panel: H&E staining, right panel: pERK staining, scale bar = 100 µm. F, Inhibition of PKC, MEK or ERK but not JNK or p38 partially rescues viability of IM treated cells. Primary keratinocytes, patient-derived SCC cells and SCC13 cells were treated for 24h with either IM alone or in combination with the PKC, MEK, ERK, JNK or p38 inhibitor. Viability was assessed by MTT assay. Graphs show mean and SD of at least three independent experiments. Data were analyzed by one-way ANOVA followed by Dunnett's multiple comparison test. * = p<0.05, ** = p<0.01, *** = p<0.001, **** = p<0.0001.

Figure 5. *IL13RA2* and *IL1R2* are involved in the mechanism of action of IM. A, *IL13RA2* and *IL1R2* gene expression is upregulated by IM treatment in a PKC/MEK/ERK -dependent manner. Cells were treated either with IM alone or in combination with the indicated kinase inhibitors for 24h followed by RNA isolation and gene expression analysis by qPCR. Data of at least three independent experiments were analyzed by

one-way ANOVA followed by Dunnett's multiple comparison test. * = p<0.05, ** = p<0.01, *** = p<0.001, **** = p<0.0001 . B, *IL13RA2* and *IL1R2* are PKCδ-dependent. SCC13 cells were transfected with siRNA against PKCδ and treated for 24h with 100 nM IM. Cell viability was assessed by MTT assay. C, Knock-down of *IL13AR2* and *IL1R2* partially rescues viability of IM treated cells. SCC13 cells were transfected with two different siRNA against *IL13RA2* or *IL1R2* followed by 24h of IM treatment. Viability was assessed by MTT assay. All graphs (B, C) show mean and SD of three independent experiments. Data were analyzed by Student's t-test. * = p<0.05, ** = p<0.01, *** = p<0.001, **** = p<0.0001.

Figure 1

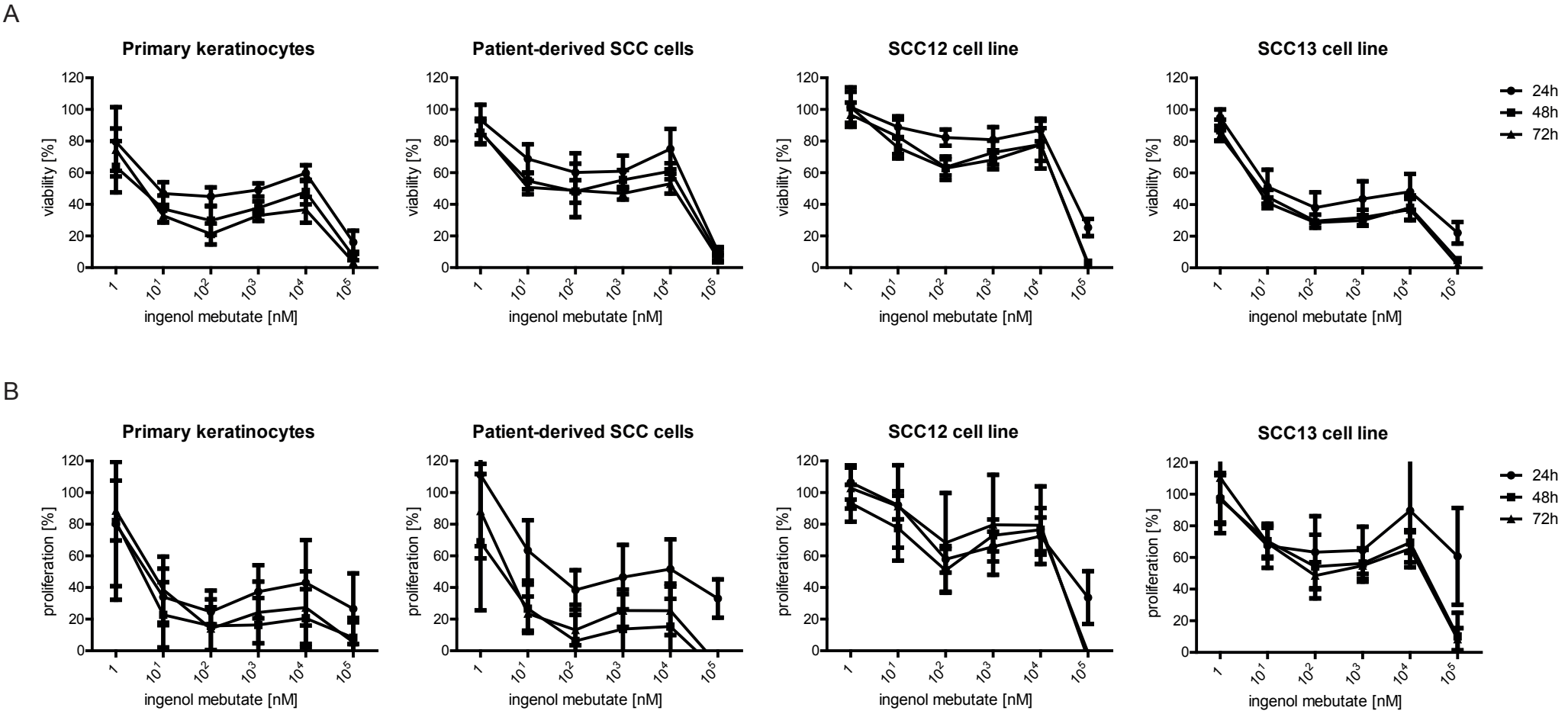

Figure 2

A

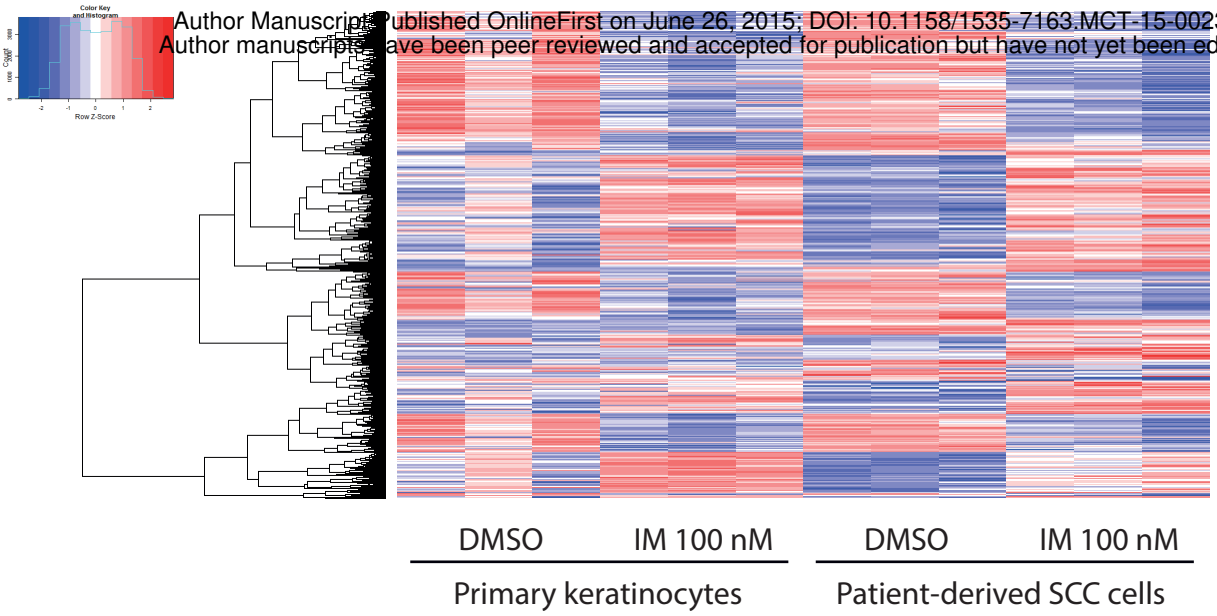

B

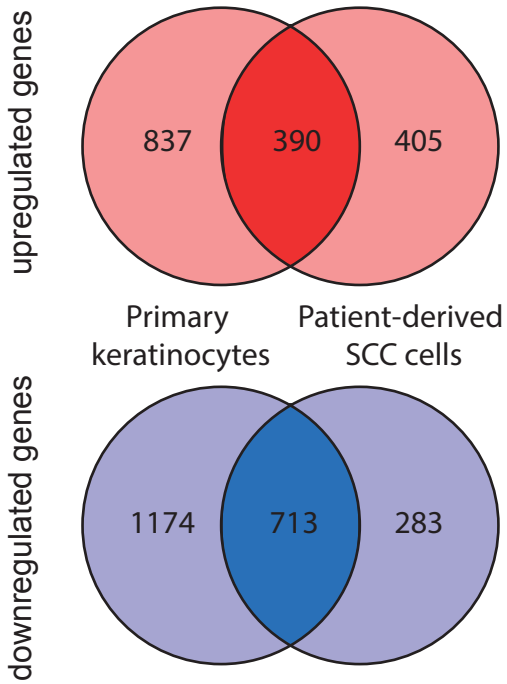

Figure 3

A

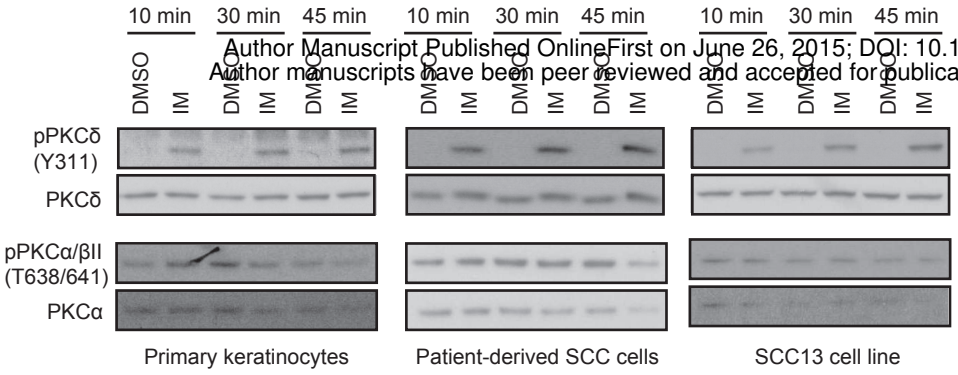

B

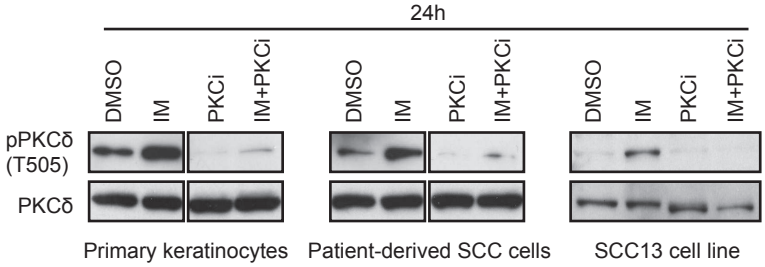

C

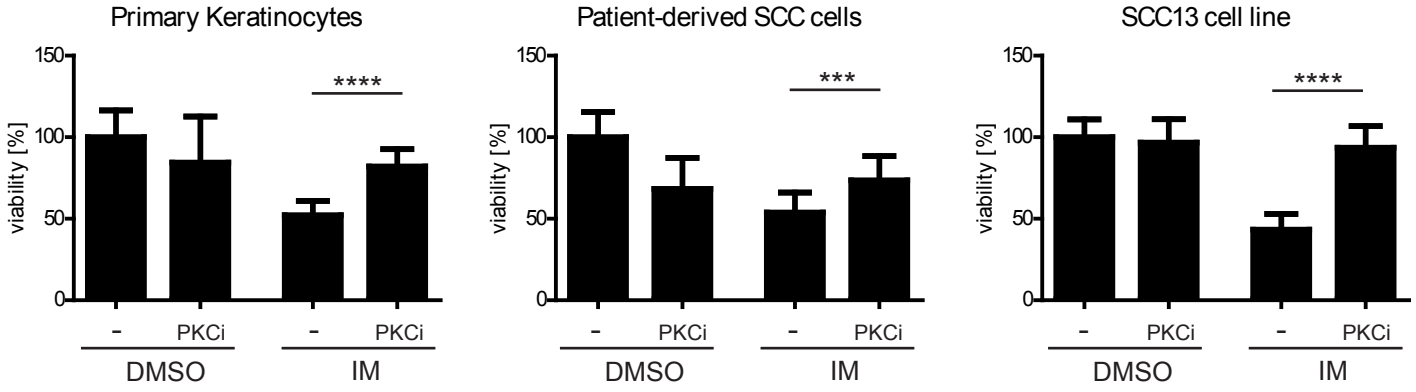

D

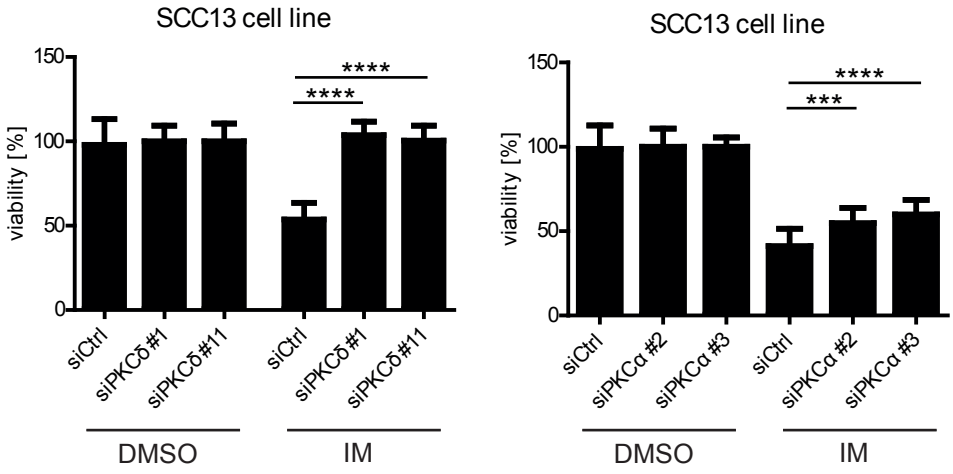

Figure 4

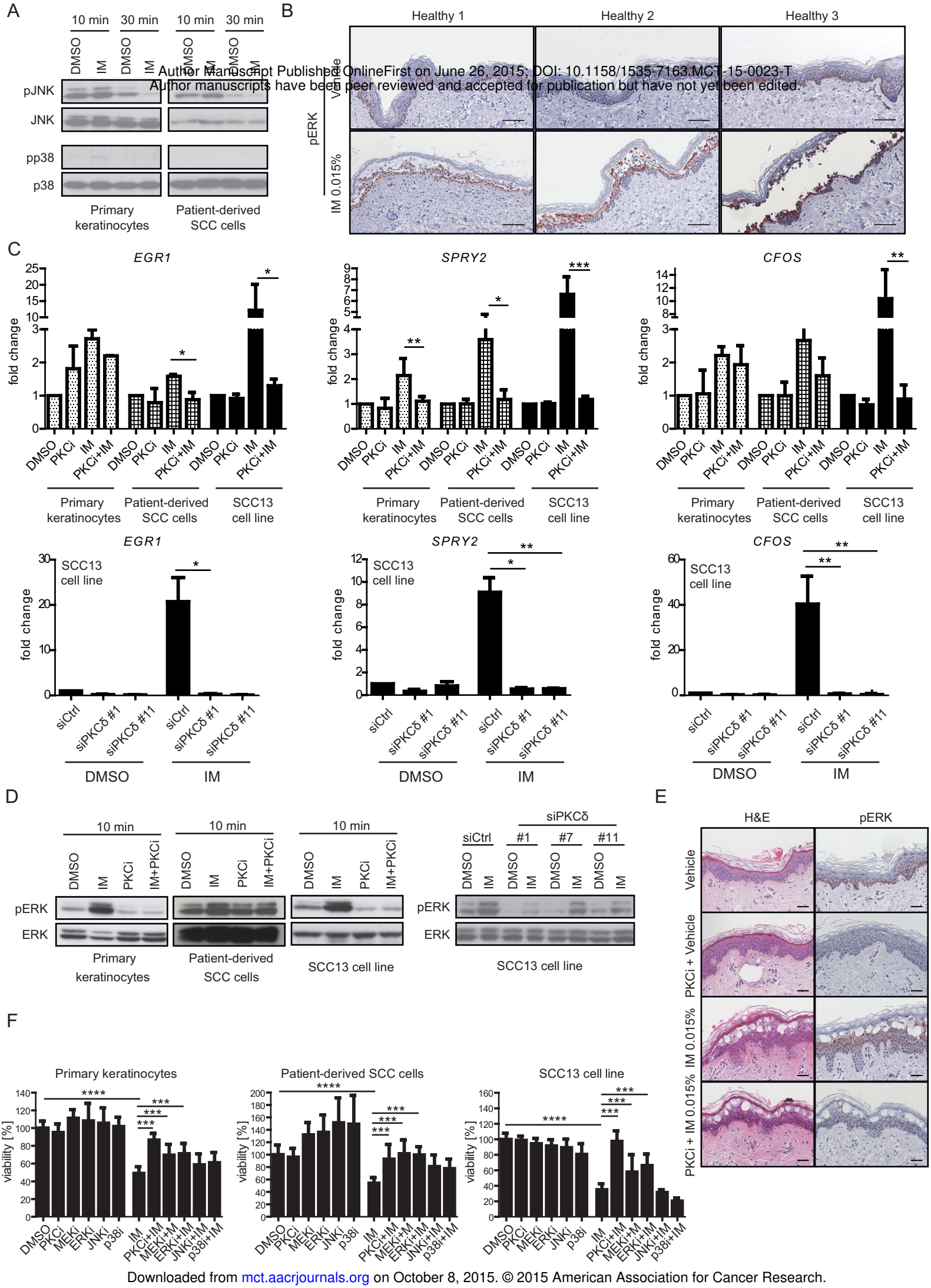

Figure 5

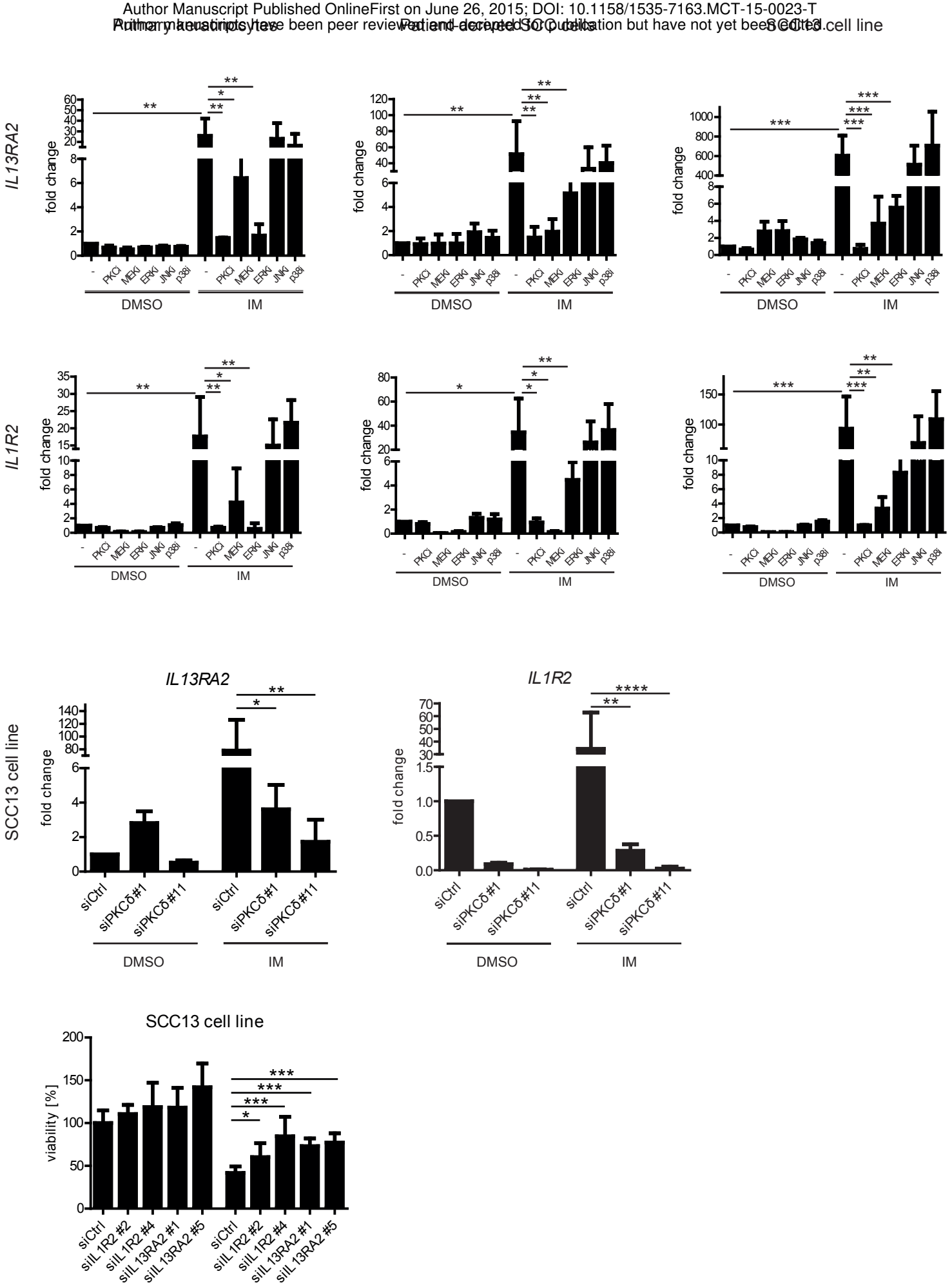

AACR American Association for Cancer Research

Molecular Cancer Therapeutics

Ingenol mebutate signals via PKC/MEK/ERK in keratinocytes and induces interleukin decoy receptors IL1R2 and IL13RA2

Sandra N. Freiberger, Phil F Cheng, Guergana Iotzova-Weiss, et al.

Mol Cancer Ther Published OnlineFirst June 26, 2015.